Riverbed dune morphology of the Lowermost Mississippi River – Implications of leeside slope, flow resistance and bedload transport in a large alluvial river

Shuaihu Wu [1,2,3], Y. Jun Xu[1,4]*, Bo Wang[1], Heqin Cheng[3]

[1] School of Renewable Natural Resources, Louisiana State University Agricultural Center, 227 Highland Road, Baton Rouge, LA 70803, USA

[2] State Key Laboratory of Hydroscience and Engineering, Tsinghua University, Beijing 100084, China; wushuaihuxiaolaoda@163.com

[3] State Key Lab of Estuarine & Coastal Research, East China Normal University, Shanghai 200062, China; hqch@sklec.ecnu.edu.cn

[4] Coastal Studies Institute, Louisiana State University, Baton Rouge, LA 70803, USA

* Corresponding author: Y. Jun Xu (yjxu@lsu.edu)

Abstract: Dunes are critical for understanding riverine sediment transport, deposition, flow resistance and channel flow processes. Although previous studies have examined the riverbed micromorphology of the Lower Mississippi River in the USA, our knowledge of detailed quantification of dune morphology in this and other large alluvial rivers is still limited. It is also not well understood how dunes in a straight reach and a meander bend differ in their characteristics, as well as how dune morphology may have been affected by human activities (i.e., river engineering). In this study, we utilized multi-beam bathymetric measurements over four 1.6-8.0 km long reaches in the Lowermost Mississippi River (LmMR) to analyze riverbed micromorphologic features. Three of the four reaches were located in the upper part of the LmMR between river kilometers (RK) 474-477, 483.6-485.2 and 491.7-493.3, and the other reach was located in the lower part, between RK 120 and RK 128. We analyzed a total of 3,258 dunes in these river reaches and found large dunes were dominant. These dunes were characterized by low mean leeside slope angle (10.8°), indicating flow resistance caused by dunes may be smaller. When compared with dunes in the straight reaches, dunes in the meander bends were much larger (1.06 m vs. 0.81 m) and had a higher bed roughness (0.91 vs. 0.68), which may be related to the varied flow velocity. Dune size increased with increasing water depths across the river channel of a straight reach, while it decreased with increasing water depths across the river channel of a meander bend. When compared with the dunes in the lower-river reach, the dunes in the upper-river reach were significantly higher in height and shorter in wavelength, and showed much higher bed roughness (1 vs. 0.68), which may be closely related to the larger riverbed slope and grain size of bed sediment occurred in the upper-river reach, as well as a combined effect of the Old River Control Structure (RK 500) and backwater effect.

These findings indicate the strong impact of turbulent flow, slope and sand source on dune formation and riverbed deposition.

Keywords: River dunes; Fluvial geomorphology; Channel morphology; River bedform; Meandering bend; Multi-beam profiling; Mississippi River

1. Introduction

Dunes with rhythmic patterns in alluvial river channels are the most common bedform. They are generally formed in a sandy deposit segment where the mean grain size of materials is larger than 125 μm (Wu et al., 2009). Dunes can significantly influence flow structure, therefore affecting sediment transport (Knaapen et al., 2001; Parsons et al., 2005; Naqshband et al., 2016). In return, the geometry of dunes is an essential component in determining flow resistance and water levels for flood management purpose (Karim, 1999). Therefore, understanding the formation and morphology of dunes can be important regarding river management for navigation, flood control, and understand the distribution of riverine sand (Amsler and Garcia, 1997; ASCE Task Force, 2002; Best and Kostaschuk, 2002; Best, 2005; Besio et al., 2008).

A number of studies have detailed mechanisms of dune growth and forms in various alluvial rivers. Kostaschuk and Villard (1996) found that long, low-angle leesides are formed by sediment deposition in dune troughs, and that dune symmetry and crest rounding of symmetric dunes are related to high sediment transport rates. Dunes with lobe or saddle-shaped crest lines can create larger and more structured areas of vertical velocity with smaller separation zones than two-dimensional straight-crested dunes (Parsons et al., 2005). In the Columbia River, dunes with separated flow occurred when bedload dominated sediment transport, while dunes without flow separation occurred when suspension transport was the dominant transport mechanism (Smith and McLean, 1977). In a recent study, Cisneros et al. (2020) quantified shapes of dunes by bathymetric data in several large rivers in the world. They found that most of the dunes in these rivers have low-angle leesides and the dune height is usually less than 10% of the local

flow depth. However, few studies have investigated the morphology and dynamics of dunes in the backwater reach of a large alluvial river, especially comparing characters of dunes in the reaches with different bed slopes and curvatures.

The Mississippi River (Figure 1) drains approximately 3.2 million km^2, extending over approximately 42% of the contiguous United States and adjacent areas of Canada. It is the seventh-largest river in discharge and sediment load in the world (Syvitski and Milliman, 2007), is also the major source of fresh water, sediment, nutrients, and terrestrial organic carbon to the northern Gulf of Mexico (Milliman and Farnsworth, 2011). Commonly, the reach from the confluence of the Mississippi River with the Ohio River to the Gulf of Mexico is referred to as the Lower Mississippi River. In the publications (e.g., Mossa, 1996; Nittrouer et al., 2011a and b; Joshi and Xu, 2015; Wang and Xu, 2015 and 2018), the term "Lowermost Mississippi River (or LmMR)" has been used for the last 500-km river reach from the Mississippi-Atchafalaya river diversion (also known as the Old River Control Structure) to the Gulf of Mexico outlet (Figure 1). The Old River Control Structure (ORCS) located at river kilometer (RK) 500 (i.e., the distance upstream of the Gulf of Mexico outlet) was constructed by the U.S. Army Corps of Engineers in 1963, which diverts 24% of the Mississippi River into the Atchafalaya River on average in the recent decades (Wang and Xu, 2020). The location is a historic avulsion point of the Lower Mississippi River.

The LmMR is a typical case whose channel is affected by backwater effects and human interventions (i.e., complicated river engineering). The reach is generally considered as a lifeline that provides sediment to the Mississippi River Delta. Since 1932, the Mississippi River Delta has lost about 4.877×10^3 km^2 coastal land mainly due to the reduced sediment supply to the floodplain (Couvillion et al., 2011). The Louisiana Coastal and Protection Restoration Authority

has proposed to build several large sediment diversions in the Lower Mississippi River (CPRA, 2017). It is, therefore, ultimately important to understand sediment transport in the river for current delta protection and restoration. However, sediment transport in the LmMR is complicated and not well understood. A 1-D modeling studied by Nittrouer et al. (2012) showed that the channel bed in the LmMR tends to aggrade between RK 500-150 and degrade between RK 150 and 0. Wang and Xu (2018) also found that ~70% of riverine sand could have deposited in the reach of RK 500-150 during 1992-2013. However, for a better understanding of sediment transport in the river, further detailed 2-D/3-D hydrodynamic modeling of the whole LmMR is needed. Wang and Xu (2018) pointed out that the 1-D modeling has difficulties in actual sediment transport due to emerged channel bars and meandering pattern of the river. Such modeling work (2-D/3-D hydrodynamic modeling) cannot succeed without detailed dune information which is critical for determining bed roughness and resistance in modeling studies (Karim, 1995; Best, 2005).

Previous studies found that channel-bed aggradation occurred in the upper backwater reach of the Mississippi River from RK 500 to RK 150, while the final 150-km reach experienced channel-bed erosion (Nittrouer et al., 2012; Wang and Xu, 2018). Consequently, the LmMR can be divided into the upper reach (uLmMR) (RK 150-500) and the lower reach (ILmMR) (RK 0-150). In their studies on bedforms along the last 150-km channel of the Mississippi River, Nittrouer et al. (2008 and 2011a) found that straight reach segments were normally covered by dunes on the entire bed, while bends were typically areas devoid of alluvial covers. Characteristic dune size on the channel bed at RK 45 was reported to be 0.54–0.91 m in height and 15.00–24.00 m in wavelength (Nittrouer et al., 2011a). The wavelength-to-height ratios were 17.3–44.4, and both dune height and wavelength increased with water depth. From a recent study

on dynamic links between sediment supply and transport, Ramirez and Allison (2013) reported that the largest dunes located near the thalweg (30–40 m water depth) between RK 75 and RK 100 of the LmMR. These studies focused on the lLmMR (i.e., below RK 150). To our best knowledge, little reports exist on the morphology of riverbed dunes in the uLmMR closer to the river diversion structure, the Old River Control Structure.

In three recent studies, Joshi and Xu (2015) and Wang and Xu (2016 and 2018) reported that riverbed in the very uLmMR had been aggrading at a fast space, attributing it to the flow reduction downstream of the ORCS. In another recent study on bedload material transport around the ORCS, Wang and Xu (2020) found that on the mainstem Mississippi, the percentage of bed material diversion (83%) is larger than the percentage of flow diversion (76%), resulting in the diversion channel receiving a disproportionate amount of flow (24%) relative to bed material supply (17%). Consequently, severe bed scouring occurred in the controlled Outflow Channel to the Atchafalaya River, while riverbed aggradation progressed in the mainstem Mississippi downstream of the diversion structures. While evidence is amounting on the diversion effect on sediment transport in the upper LmMR, it was not clear how the river channel bedform may have been affected by the river engineering.

Flow velocity in river meander bends has been investigated intensively in the past four decades (e.g., Smith and McLean, 1984; Odgaard and Bergs, 1988; Johannesson and Parker, 1989; Hsieh and Yang, 2003; Termini and Piraino, 2011). In a recent study, Liu and Bai (2014) reported that besides the primary flow in the streamwise direction for bends, there is a helical flow across the section due to the channel meander. This helical flow goes from the inner bank towards the outer bank near the water surface, and from the outer bank towards the inner bank near the channel bottom, leading to a circular flow at the cross section of the meandering channel

bend. This may influence the distribution of riverine sand at the cross section of the bend. The distribution of riverine sand of a channel was closely with the dune characteristics. Consequently, studies focused on dune characteristics at different locations of a channel in the LmMR can contribute to understanding the distribution of riverine sand. However, few studies have focused on riverbed dune morphology of meander bends.

In general, there is a knowledge gap on how dunes change within a river reach between straight and curved sections, and between areas with different slopes along the backwater reach of large alluvial rivers such as the Mississippi River. A study focusing on dunes in the Mississippi River can be crucial for improving our understanding of the distribution of riverine sand and modeling sediment transport in the Mississippi River as well as other alluvial rivers around the world.

In this study, we used recent high-resolution multi-beam measurements on the riverbed in the upper and lower reaches of the Lowermost Mississippi River to assess dune formation in straight and bend segments, and the hydrographic survey data obtained by the single beam measurements were used to assess morphological changes of riverbed in the upper and lower reaches of the LmMR. Specifically, the study aimed to 1) characterize the bedforms in four reaches along the LmMR; 2) investigate the difference of dunes developed in the upper (close to the Mississippi – Atchafalaya River diversion structure) and lower reaches of the LmMR, which differ in riverbed slopes; and 3) analyze the differences in dune characteristics in the straight and bend segments of the river; and 4) compare the dune morphology in different water depths across the river channel of the straight reaches and meander bends. The primary goal is to improve our understanding of characteristics and morphological responses of river dunes to flow conditions in

large alluvial rivers. The results from the study can also be helpful to understand the interactive relationship between dune morphology and human interventions.

2. Methods

2.1. Study area

The area of the present study includes four reaches of the LmMR, namely at RK 474-477, 483.6-485.2, 491.7-493.3, and 120-128 (Figure 1 and Table 1). The three upper reaches are located shortly downstream (23-26 km, 14.8-16.4 km, and 6.7-8.3 km) of the ORCS (RK 500) and could show typical bedforms affected by the river engineering and backwater effects. The selected lower reach has been rarely dredged. Therefore, it could be a typical reach for the lower segment of the LmMR mainly controlled by backwater effects. These reaches include straight channels (RK 120-122 and RK 483.6-485.2) and meander bends (RK 122-128, 474-477, and 491.7-493.3) (Table 1). Previous studies have investigated the grain size of bed sediment (Table 2) in different reaches of the LmMR (Nittrouer et al., 2008 and 2011a; Ramirez and Allison, 2013; Knox and Latrubesse, 2016). Knox and Latrubesse (2016) reported that median grain size of sediment collected in 2012 varied between 181 and 483 μm in the uLmMR (Table 2). Ramirez and Allison (2013) found that the bed material collected in 2010 was dominated by sand and had a mean and median grain size in the range of 150-350 μm in thelLmMR.

The mean annual suspended sediment discharge at Tarbert Landing gauging station (RK 493) for the period 1980-2010 was 127 MT, about one-third of which was discharged when the river was at an intermediate stage, a NOAA-defined river initial flood stage of 12.1 m for the location, river discharge between 18,000 - 25,000 m^3/s; more details can be found in Rosen and Xu (2014). Seasonally, discharge of the LmMR is high (i.e., 22468 m^3/s) during the winter and spring

(January-May) and low (i.e., 8171 m^3/s) during the summer and early fall (July-November). Therefore, sediment discharge of the LmMR varies widely with flow (Meade and Moody, 2010; Rosen and Xu, 2014) and downstream locations (Joshi and Xu, 2017). It was maximized in the discharge ranging between 18,000 and 32,000 cms, accounting for near 50% of the total annual sediment yield (Rosen and Xu, 2014). The suspended sediment concentration at Tarbert Landing increases nonlinearly with discharge (Rosen and Xu, 2014; Joshi and Xu, 2015), and about 27 MT of the annual TSS delivery were found to be coarser grain-size sediment (Joshi and Xu, 2015). In a bedload modeling study, Joshi and Xu (2017) estimated an annual bedload rate of 7 MT for Tarbert Landing at RK 493 and of 8 MT for Baton Rouge at RK 368. Because of the very flat landscape, tides from the Gulf of Mexico could penetrate 350-400 km upstream the LmMR during low flows (September - October) and < 50 km during high flow (February - June), but the tidal currents are normally too weak to reverse the river flow (Allison and Meselhe, 2010).

2.2 Data collection and analysis

This study utilized bathymetric survey data collected by the U.S. Army Corps of Engineers (USACE) during 22-29 March, 4-15 April, and 2-23 October 2012, using a Reason 7101 swath bathymetry profiler. Calibrations of pitch, roll, and yaw were conducted, and position, heading, and velocity information were provided by a dual antenna differential GPS. The vertical resolution of the multi-beam instrument was 1.5 cm. The hydrographic survey data of the LmMR were collected by the USACE during 1992, 2004 and 2013, using single beam fathometer. In each survey dataset, there were approximately 2000 cross-sections in a distance of about 30 m apart. River widths were determined as the distance from right to left bank during bankfull discharge.

240 The collected multi-beam data were post-processed by using CARIS HIPS 7.1 software,
241 and the navigation drop-outs, multiples, and other noise were removed. The processed multi-
242 beam data were then imported into the ArcGIS 10.3 (ESRI, Redlands, CA) platform and the
243 dimensions of each dunes at a resolution of 0.6 m by 0.6 m grid were determined through
244 creating Digital Elevation Model (DEM) with the software (Figure 2). In the ArcGIS 10.3
245 platform, the DEM was created with the inverse distance weighted interpolation (a spatial
246 interpolation technique) of the hydrographic survey data in a resolution of 10 m by 10 m grid.
247 The morphological changes of the riverbed cross-sections were analyzed through subtracting the
248 riverbed elevation between 1992 and 2013. The riverbed slope was calculated by using the
249 hydrographic survey data. The profile of the riverbed dunes was extracted based on the vertical
250 direction of the dune ridge crest (Figure 2). In general, dunes have irregular size and shape and
251 were described by wavelength and height. The wavelength (L) and height (H) of the dunes can
252 be calculated using the Knaapen's (2005) reliable approach:

253 $$L = L1 + L2 \quad (1A)$$

254 $$H = H1 \quad (1B)$$

255 where $L1$ was defined as the distance between the downstream trough and crest, $L2$ was defined
256 as the distance crest and upstream trough, and H was defined as the difference ($H1$) of the bed
257 elevation between the leeside trough and the crest (Figure 3). The mean wavelength and mean
258 height were estimated by averaging multiple dune length and dune height, respectively. The
259 frequency distribution and cumulative percentage of dune height and dune wavelength were
260 analyzed with Excel software (Microsoft Office 2016, Microsoft Co.). Based on the
261 classification scheme developed by Ashley (1990), dunes can be divided into four
262 distinguishable populations: very large dunes (＞100 m in length), large dunes (10–100 m in

length), medium dunes (5–10 m in length) and small dunes (0.6–5 m in length). Paired Student's t-test was utilized to compare differences in dune characteristics between different reaches. The level of statistical significance was generally considered as $p<0.05$.

2.3 Bed roughness associated to dunes

Bed roughness (*ks*) of a river channel is mainly affected by form drag in sand, gravel, or sand-gravel bed rivers (Paarlberg et al., 2010). To examine the spatial distribution of bed roughness, we estimated *Ks* associated with dune dimension using the Van Rijn's (1984) approach:

$$Ks = 1.1\, H_D\, (1 - e^{(-25\, H_D/L_D)}) \qquad (2)$$

where H_D is the mean dune height in m, and L_D is the mean dune length in m.

3. Results

3.1. General riverbed morphology of the LmMR

In the LmMR, the studied 3,258 dunes varied from 0.02 to 6.69 m in height with an average of 1.01 m, and from 2.96 to 129.54 m in wavelength with an average of 16.79 m, yielding a height to wavelength ratio ranging from 0.002 to 0.252 (Figure 4 and Table 3). There were 1330 dunes developed in the RK 120-128 of the lLmMR, and there were 1010, 354 and 564 dunes in the RK 474-477, RK 483.6-485.2 and RK 491.7-493.3 reaches, respectively, in the uLmMR. The mean leeside slope angle (10.8°) of these dunes was significantly larger than the mean stoss side slope angle (5.76°) of dunes in the study reaches, with leeside slope angles between 0.18° and 47.11°, and stoss slope angles between 0.32° and 31.64° (Table 3). The mean ratio of stoss side slope to leeside slope was 0.58 which indicates these dunes are nearly highly asymmetric.

Four distinguishable populations of dune size were observed in the study reaches of the LmMR: very large dunes, large dunes, medium dunes, and small dunes. Very large dunes counted only 0.12%; large dunes (10–100 m in length) appeared predominantly, i.e., 70.3%; medium dunes made up 27.5%; and small dunes represented 2.1% of all 3,258 studied dunes. Dunes with a height of 0.2–2.3 m and with a length of 5–33 m (a larger proportion) made up 92.82% and 89.93%, respectively, of all the observed dunes (Figures 5a and 5b).

3.2. Difference between upper and lower-river reaches and between straight reaches and meander bends

When compared with the dunes in the lower-river reach (i.e., an average height of 0.87 m and an average length of 17.62 m), the dunes in the upper-river reach were obviously higher (i.e., an average height of 1.11 m) and shorter (i.e., an average length of 16.21 m) (Table 3 and Figures 6, 7a and 7b). In the upper-river reach, dunes with a height of 0.2–2.3 m and with a length of 5–33 m amounted to 90.56% and 86.77%, respectively, of all 1928 observed dunes (Figures 6a and 6b). In the lower-river reach, dunes with a height of 0.2–2.3 m and with a length of 5–33 m amounted to 96.09% and 94.51%, respectively, of all 1330 observed dunes (Figures 6c and 6d). The results indicate a significant difference in the dune height (p<0.0001) and dune wavelength (p=0.0007) between the upper reach and lower reach of the study area (Table 4).

Compared with the dune form index (height/wavelength) in the lower-river reach (i.e., 0.049), the values of these dunes in three upper-river reaches (RK 474-477, 483.6-485.2, and 491.7-493.3) were obviously higher (i.e., 0.072, 0.073 and 0.072) (Figure 7e). There is a significant difference (p<0.0001) in the dune form index between the upper reach (i.e., 0.073) and lower reach (i.e., 0.049) (Table 4).

306 Compared with the mean stoss slope angle (i.e., 4.21°) of the dunes in the lower-river reach,
307 the values of these dunes in three upper-river reaches (RK 474-477, 483.6-485.2, and 491.7-
308 493.3) were obviously higher (6.92°, 6.73°, and 6.72°) (Figure 7c). The dunes in the upper-river
309 reaches also showed obviously higher mean lee slope (11.47°, 12.55°, and 12.1°) and ratios of
310 mean stoss side slope to mean leeside slope (i.e., 0.66, 0.58 and 0.61) than the dunes in the
311 lower-river reach (i.e., 9.40° and 0.52) (Figures 7d and 7f). There is a significant difference
312 (p<0.0001) in the symmetrical characteristic (stoss side slope / leeside slope) of dunes between
313 the upper reach (i.e., 0.64) and lower reach (i.e., 0.52) (Table 4).
314 Comparing dunes developed in the straight segments and bends, we found there is a
315 significant difference (p<0.0001) in dune size (Table 5). Much smaller dunes (i.e., an average
316 height of 0.81 m and an average length of 14.27 m) developed in the straight reaches, while
317 larger dunes (i.e., an average height of 1.06 m and an average length of 17.40 m) occurred in the
318 bends (Table 3). In both straight reaches and bends, approximately 90% of the dunes were 0.2–
319 2.3 m in height and 5–33 m in length (Figure 8). With respect to larger dunes (i.e., >2.3 m in
320 height or >33 m in length), the amounts of dunes in the bends was obviously higher than that in
321 the straight reaches (i.e., 6.19% vs. 3.43% or 8.75% vs. 4.83%, respectively) (Figure 8).
322 Compared with the mean ratio of stoss side slope to leeside slope (i.e., 0.48) of these dunes in the
323 bends, the value in the straight segments was obviously higher (i.e., 0.61). There is a significant
324 difference (p<0.0001) in the symmetrical characteristic (stoss side slope / leeside slope) and the
325 geometry of dunes (dune height to dune length) between the straight reaches and bends of the
326 study area (Table 5).
327 Dune size varied with the water depths across the river channel in the LmMR. Much larger
328 dunes occurred in the deeper portions across the river channel in the straight reaches, while much

329 smaller dunes developed in shallow waters near the bank. The water depths used here were
330 recorded depth at the time when the bathymetric surveys were conducted. For example, the
331 largest dunes near the thalweg (i.e., 26–30 m water depth) ranged from 19.74 m in length and
332 1.02 m in height (Table 6). Conversely, larger dunes were formed in the shallower waters across
333 the river channel in the bends, while smaller dunes were formed in the deeper meander bend
334 thalweg. For example, the largest dunes closest to the bank (i.e., 17–19 m water depth) ranged
335 from 29.33 m in length and 1.29 m in height. The smallest dunes situated between 25–27 m
336 ranged from 13.7 m long and 0.64 m high (Table 6).

337 *3.3 Dune roughness*

338 The bed roughness (*ks*) associated with the dunes varied between 0.40 and 1.0 (Tables 3 and
339 6). When compared with dunes in the lower-river reach (0.68), dunes in the upper-river reaches
340 showed a much higher value of *ks* (1.0). Compared with dunes in the straight reaches, dunes in
341 the bends showed much higher *ks* (0.91 vs. 0.68). For the straight reaches, the obviously higher
342 value of *ks* (0.81) occurred in the deeper portions across the river channel, while the much
343 smaller value of *ks* (0.40) occurred in the shallow waters area. Conversely, the values of *ks*
344 decrease with increasing water depths across the river channel in the bends. The highest value of
345 *ks* (0.95) occurred in the shallow waters of the bends, while the lowest value of *ks* (0.49)
346 occurred in the thalweg of the deeper meander bends.

347 *3.4 Riverbed slope and riverbed elevation change*

348 Compared with the riverbed slope (0.38‰) of the lower-river reach of the study area (RK
349 120-128), obviously higher slope (0.95‰, 2.2‰ and 3.2‰) occurred in the three upper-river
350 reaches (RK 474-477, 483.6-485.2 and 491.7-493.3, respectively). Cross-sections A, B, and C in

the uLmMR all showed that the riverbeds have experienced considerable aggradation over the past two decades (Figure 9), with the maximum accretion of 12 m, 8.8 m, and 3 m during 1992-2004, respectively, and with the maximum accretion of 5 m, 3.8 m, and 9 m from 2004 to 2013, respectively. Cross-sections D and E in the lLmMR showed that the riverbeds experienced slight erosion (Figure 9), with the maximum erosion of 2 m and 3 m during 1992-2013, respectively.

4. Discussion

4.1 Mechanisms for the dune morphology of different locations

The detailed analysis of dune shapes in this study illustrates that in a large river, the dunes have significantly different features depending on their locations, i.e., upstream vs. downstream, straight reach vs. bend. The occurrence, morphologic features, and development of river channel dunes depend mainly on river flow velocity, water depth, and sediment grain size (Hu, 2005).

Rosen and Xu (2014) reported that mean annual suspended sediment load of approximately 120 million tonnes (MT) from 1980 to 2010 were delivered into the LmMR. Joshi and Xu (2015) found that mean annual sand load of about 27 MT during 1973-2013 were transported into the LmMR. These provided a basic source of sands for development of dunes in the LmMR. Larger riverbed slope may result in channel incising, which may contribute to the coarsening of sediment and result in larger dunes (Southard and Boguchwal,1990). The riverbed slope (0.95‰, 2.2‰, and 3.2‰) in the upper-river reach of the study area was obviously larger than the lower-river reach (0.38‰). This may result in the larger grain size of bed sediment occurred in the upper-river reach of the study area. Previous studies have also shown the mean grain size of bed sediment (Table 2) decreases downstream in the Lower Mississippi River (Nittrouer et al., 2008; Nittrouer et al., 2011a; Ramirez and Allison, 2013; Knox and Latrubesse, 2016). Consequently,

these may be closely related to the much higher dunes (i.e., 1.15 m, 0.90 m, and 1.16 m, respectively) developed in the three upper reaches of the LmMR (Table 3 and Figure 7a).

The larger dune size in the upper LmMR may have also been a result of riverbed aggradation downstream of the Old River Control Structure (RK 500). By diverting approximately 25% of the Mississippi River into the Atchafalaya River, the ORCS reduce the flow velocity, which has caused substantial aggradation of the riverbed (Wang and Xu, 2018) and the growth of three large emerged channel bars in a 10-km reach downstream of the ORCS over the past three decades (Wang and Xu, 2016). Nittrouer et al. (2012) also demonstrated the tendency for channel-bed aggradation in the upper backwater reach of the Mississippi River (RK 150-600), while channel-bed erosion occurred in the final 150 km reach. Our study found the riverbeds in the uLmMR from RK 493 to RK 474 have experienced considerable aggradation over the past two decades (Figures 9A-C), while the riverbeds in the lLmMR showed erosion (Figures 9D and 9E). These findings are in good agreement with those recently reported by Joshi and Xu (2017), and the upstream aggradation may be the result of a combined effect of flow reduction due to the river diversion at the ORCS and backwater effect as discussed by Wang and Xu (2018). Wu et al. (2020) found that dune size was impacted by backwater hydrodynamics in the lowermost 410 km of the Mississippi River. This finding and our study complement each other. These may have been a major factor for the much higher dunes (i.e., an average height of 1.11 m) and longer dunes (i.e., an average length of 17.62 m) found in the upper-river reach and lower-river reach (Table 3), respectively. The results showing a significant difference in the dune geometry (ratios of dune height to dune length) and dune symmetry (ratios of stoss side slope to leeside slope) between the upper reaches and lower reaches of the study area. These suggested that the impact of slope and sand source on the dune structure.

Duan and Julien (2010) reported that flow characteristics in a meandering channel are different from those in a straight channel. Variations of current thickness and streamwise velocity across the channel normally increase with increasing channel curvature (Das et al., 2004). Blanckaert and Graf (2001) reported the downstream velocity in the outer half-section of the bend is higher than the one in the straight uniform flow. Dunes are observed to grow rapidly with increasing flow strength (Naqshband et al., 2014). In a recent modeling study, Zhou and Endreny (2020) demonstrated that hydraulic complexity gets lost when a river meander is modified from curvature to straightened. Therefore, compared with the dunes in the straight reaches (i.e., an average height of 0.81 m and an average length of 14.27 m), the observed much larger dunes (i.e., an average height of 1.06 m and an average length of 17.40 m) (Table 3) developed in bends may closely related to the varied flow velocity between straight reaches and bends.

Classic bedform features in meanders include point bars on the inner bank and pools along the outer bank centered at the meander bend apex, and riffles upstream and downstream of the bend (Leopold and Wolman, 1960; Wohl, 2020). Due to the influence of the helical flow, a circular flow occurred in the cross section of the meandering channel (Liu and Bai, 2014). Consequently, large channel incision and bed scour mainly occur in the outer bank forming a deeper channel, while sediment deposit on the inner bank (shallow waters) of the bends. This could have caused dune size to decrease with increasing water depths across the river channel of the bends (i.e., from the inner bend to the outer bend). Nittrouer et al. (2011b) reported that substrate was exposed in the channel thalweg of the last 165-km LmMR, particularly in meander bends, which suggested sediment was lesser in deeper portions of meander bends. Wu et al. (2005) reported that sufficient sediment is the foundation for dune development. This implies

419 that the scale of dunes may be smaller in deeper portions of a meander. For example, much
420 larger dunes (i.e., an average height of 1.29 m and an average length of 29.33 m) developed in
421 the shallow waters (i.e., 17-19 m water depth) or inner bend, while much smaller dunes (i.e., an
422 average height of 0.64 m and an average length of 13.7 m) occurred in the deeper portions (i.e.,
423 25-27 m water depth) or outer bend (Table 6).

424 In terms of the relationship between dune size and flow depth, a previous study reported that
425 in straight reaches, dune size gradually increased with increasing water depths of the channel in
426 the Yangtze River Estuary (Li et al., 2008). Wu et al. (2010) found the most favorable area for
427 dune development was near 30-m water depth in the Yangtze River. In our study, large dunes
428 (i.e., an average height of 1.02 m and an average length of 19.74 m) in the LmMR were mainly
429 found in the deeper water locations (i.e., 26–30 m water depth) across the river channel of the
430 straight reaches (Table 6). This is surprisingly consistent with the observation in the Yangtze
431 River. In addition, Wu et al. (2016) found the dunes have a low average lee slopes (<10°) in the
432 Yangtze River Estuary. Zheng et al. (2017) found the very large dunes have a low average lee
433 slopes (<5°) in the Yangtze River (i.e., the tidal reach). Cisneros et al. (2020) reported that the
434 dunes with low-angle lee slopes (<10°) were predominant in large rivers. These are also
435 consistent with our observation that the average lee slope for the dunes in different reaches of the
436 Lowermost Mississippi River is 10.8° (Table 3).

437 In the study reaches of the LmMR, the mean leeside slope angle (10.8°) of these dunes
438 (n=3258) was considerably larger than the mean stoss side slope angle (5.76°) of dunes (Table 3),
439 which indicated the steep slopes of asymmetrical dunes facing predominantly downstream
440 because of the micro-tidal environment (the diurnal stage range was about 30 cm) in the Gulf of
441 Mexico (Nittrouer et al., 2008) and the dune geometry was mainly controlled by the river flow.

Flow acceleration /deceleration and flow separation related to the asymmetrical dune morphology of the LmMR can generate form drag (a net force), which is crucial in assessing energy expenditure and flow resistance (Maddux et al., 2003). Compared with classic angle-of-repose dunes, dunes with low leeside slope angle will produce less turbulence, which reduces flow resistance generated by dune form roughness (Cisneros et al., 2020). These dunes were characterized by low mean leeside slope angle (10.8°) in the study reaches of the LmMR, indicating flow resistance caused by dunes may be smaller.

4.2 Implications of the dune morphology

The generation of transverse and secondary circulation patterns in river curvature establish feedback loops between sediment transport and morphology of riverbed topography (Blanckaert and Vriend, 2004; Camporeale et al., 2007; He, 2018). Our results demonstrate that the dune shapes are also closely related to the river reach geometry in the lowermost channel of a large alluvial river (i.e., LmMR). Numerical simulation of sediment transport and riverbed deformation in such meandering channels can be extremely challenging due to the effects of bed slope, backwater, and river engineering. However, a careful consideration of bed roughness and flow resistance caused by dunes in different river reaches is important for predicting sediment transport, water depth and flood risk (Cisneros et al., 2020). For instance, for such a modeling work, the uLmMR can be given a larger flow resistance caused by the dune roughness (Ks = 1.0) due to large bed slope and coarser sediment, while the lLmMR has a lower flow resistance (Ks = 0.68) from our detailed study on dune shape. Paarlberg et al. (2010) found that dune roughness was linearly related to dune height. This may explain our finding that much higher value of ks occurred in the meander bends (0.91) and upper-river reaches (1.0) when compared with dunes in the straight reaches (0.68) and lower-river reach (0.68).

River shortenings through human interventions (i.e., man-made cutoffs) have been attempted on many alluvial rivers throughout the world. Such practices have been extensive on the lower Mississippi River during the first half of the 20th century (Winkley, 1977), which may have strongly affected sediment transport and bedform in the river reach. There is an increasing realization that loss of river curvature leads to a loss of hydraulic complexity (Vermeulen et al., 2015; Konsoer et al., 2016; Zhou and Endreny, 2020) and the associated loss of ecosystem services (McCoy et al., 1999; Kozaerek et al., 2010; Gualtieri et al., 2017). The Lowermost Mississippi River is confined by levees on both banks, leaving no possibility for further meander evolution. The river channel may have re-balanced from the river engineering, but it is unclear if such an artificial system is stable, i.e., reacting slowly to imposed changes. In the recent decade, there is an interest to restore previous river meanders and/or reduce their future loss (e.g., Kondolf, 2006; Lorenz et al., 2009; Palmar et al., 2010; Wilson et al., 2020). Our study shows the heterogeneity in morphodynamic features of dunes under a heavily engineered river, providing insights into potential bedform development for river meander restoration and protection.

River engineering in the past century including dam building, channelization, and levee construction has significantly influenced river sediment transport and deposition in lower reaches of the world's large rivers (Vorosmarty et al., 2003; Walling and Fang, 2003; Walling, 2006). The changes occurred in sediment transport may lead to morphological responses of riverbed dunes. For example, dunes were detected for the first time in the North Channel of the Yangtze River Estuary (a turbidity maximum zone) because of the construction of the Three Gorges Dam and the Qingcaosha reservoir (Wu et al., 2016). Rosen and Xu (2014) reported total suspended sediment discharge at the Tarbert Landing showed a slight, statistically insignificant increasing

trend from 1990 to 2010, which indicated dams constructed in the Mississippi River may only marginally affected dune morphology in the LmMR. However, the finding from this study that dune heights appeared to be taller in the uLmMR indicates a role that the Old River Control Structure may have played. Although current understanding of dunes' role in controlling channel-scale processes and river morphodynamics is incomplete (Unsworth et al., 2020), our results may reflect an interactive relationship between human interventions and dune morphology.

5. Conclusions

This study analyzed micromorphology of riverbeds and 3,258 dunes in the upper and lower reaches of the LmMR, as well as in the straight channels and meander bends of this large alluvial river. The study found a dominance (70.3%) of large dunes (i.e., > 10 m in length). These dunes were characterized by low mean leeside slope angle (10.8°), indicating flow resistance caused by dunes may be smaller. When compared with dunes in the straight reaches (i.e., an average height of 0.81 m and an average length of 14.27 m), larger dunes were found mainly developed in the meandering bends (i.e., an average height of 1.06 m and an average length of 17.40 m), which may be closely related to the varied flow velocity. Dune size increased with increasing water depths across the river channel of the straight reaches, while dune size decreased with the increasing water depths across the river channel of the meander bends. Compared with the dunes in the lower-river reach (i.e., an average height of 0.87 m and an average length of 17.62 m), the dunes in the upper-river reaches were significantly taller (i.e., an average height of 1.11 m) but shorter (i.e., an average length of 16.21 m), likely owing to the larger riverbed slope and grain size of bed sediment occurred in the upper-river reach, as well as the influence of river engineering (i.e., Old River Control Structure) and backwater effects. The distinctive

characteristics of river dunes show that flow regime, riverbed slope, grain size and sand source may be the main factors affecting the micromorphology of riverbed dunes. The study is helpful for understanding the distribution of riverine sand and modeling sediment transport for the Lowermost Mississippi River and other large alluvial rivers with limited site-specific data.

Acknowledgments: This study was financially supported by the U.S. National Science Foundation (award number: 1212112). The study was also benefited from a U.S. Department of Agriculture Hatch Fund project (project number: LAB94459). During the preparation of this manuscript, Shuaihu Wu was supported by an award of the China Scholarship Council (File No.201506140113) and the China Postdoctoral Science Foundation (award number: 2019M660657) and Bo Wang was supported through an assistantship of the Coastal Science Assistantship Program (CSAP) administered by Louisiana Sea Grant for the Louisiana Coastal Protection and Restoration Authority (CPRA). The statements, findings, and conclusions are those of the authors and do not necessarily reflect the views of the funding agencies. The authors thank the U.S. Army Corps of Engineers for making the bathymetric data available for this study. The authors are also grateful to two anonymous reviewers and editor, whose thoughtful comments and suggestions greatly helped improve the manuscript.

List of Figures

Fig. 1. The last 500 kilometers of the Mississippi River, also termed as the Lowermost Mississippi River (LmMR), starting from the Mississippi-Atchafalaya River diversion at the Old River Control Structure to the river's Gulf of Mexico outlet (i.e. Head of the Passes). The studied reaches included straight channels at river kilometer (RK) 120-122 and 483.6-485.2, as well as meandering bends at RK 122-128, 474-477, and 491.7-493.3. Long-term river discharge records at Tarbert Landing were used for the LmMR.

534 **Fig. 2**. Typical profile of riverbed dunes in the study reaches of the Lowermost Mississippi
535 River.
536 **Fig. 3.** General definition of riverbed dune parameters.
537 **Fig. 4**. Morphologic features of dunes in the study sites (Lowermost Mississippi River),
538 including the straight reach of upper reach (a), bends of upper reach (b), straight reach of lower
539 reach (c), and bends of lower reach (d).
540 **Fig. 5.** Frequency distribution and cumulative percentage of dune height (a) and dune
541 wavelength (b) of the 3258 studied dunes in the study sites (Lowermost Mississippi River).
542 **Fig. 6.** Frequency distribution and cumulative percentage of the dune height and dune
543 wavelength in the upper reach (a and b) and lower reach (c and d) of the study sites (Lowermost
544 Mississippi River).
545 **Fig. 7.** Average values of height (a), wavelength (b), stoss slope (c), lee slope (d),
546 height/wavelength (e), and stoss slope/ lee slope (f) for different reaches of the study sites
547 (Lowermost Mississippi River).
548 **Fig. 8.** Frequency distribution and cumulative percentage of the dune height and dune
549 wavelength in the straight reaches (a and b) and bends (c and d) of the study sites (Lowermost
550 Mississippi River).
551 **Fig. 9.** Changes of channel cross sections in the upper-river reach (A, B and C) and the lower-
552 river reach (D and E) of the study sites (Lowermost Mississippi River) from 1992 to 2013. The
553 river widths were determined as the distance from right to left bank during bankfull discharge.
554 **Lists of Tables**

555 **Table 1**. Characteristics of five study river reaches of the Lowermost Mississippi River. The
556 channel width was calculated using multi-beam sonar survey data that covered the entire river
557 channel.
558 **Table 2**. Mean/median grain size of bed sediment in the Lowermost Mississippi River (unit: μm).
559 **Table 3**. Characteristic difference in dunes in different river reaches of the Lowermost
560 Mississippi River.
561 **Table 4.** Comparison of dune size in the upper/lower reaches of the Lowermost Mississippi
562 River.
563 **Table 5.** Comparison of dune size in the straight reaches/bends of the Lowermost Mississippi
564 River.
565 **Table 6**. Characteristics of dunes in straight reaches and meandering bends of the upper and
566 lower Lowermost Mississippi River for different water depths (note: water depths are negative).
567
568

569 **References**

570 Allison, M.A., Meselhe, E.A., 2010. The use of large water and sediment diversions in the lower
571 Mississippi River (Louisiana) for coastal restoration: Journal of Hydrology (Amsterdam),
572 v. 387, p. 346-360.
573 Amsler, M.T., Garcia, M.H., 1997. Sand dune geometry of large rivers during floods: Discussion.
574 Journal of Hydraulic Engineering 123, 582-584.
575 ASCE Task Force., 2002. Flow and transport over dunes, Journal of Hydraulic Engineering 127,
576 726-728.

577 Ashley, G.M., 1990. Classification of large-scale subaqueous bed forms: a new look at an old
578 problem. Jour. sediment. petrol 1, 160-172.
579 Besio, G., Blondeaux, P., Brocchini, M., Hulscher, S.J.M.H., Idier, D., Knaapen, M.A.F.,
580 Ne´meth, A.A., Roos, P.C., Vittori, G., 2008. The morphodynamics of tidal sand waves:
581 A model overview. Coastal Engineering 55, 657-670.
582 Best, J., Kostaschuk, R., 2002. An experimental study of turbulent flow over a low-angle dune.
583 Journal of Geophysical Research Oceans 107 (C9), 3135.
584 Best, J., 2005. The fluid dynamics of river dunes: A review and some future research directions.
585 Journal of Geophysical Research 110, 1-21.
586 Blanckaert, K., De Vriend, H.J., 2004. Secondary flow in sharp open-channel bends. J. Fluid
587 Mech 498, 353-380.
588 Blanckaert, K., Graf, W.H., 2001. Mean flow and turbulence in open-channel bend. Journal of
589 Hydraulic Engineering 127, 835-847.
590 Camporeale, C., Perona, P., Porporato, A., Ridolfi, L., 2007. Hierarchy of models for
591 meandering rivers and related morphodynamic processes. Rev. Geophys 45,
592 doi:10.1029/2005RG000185.
593 Cisneros, J., Best, J., Dijk, T.V., Almeida, R.P.D., Amsler, M., Boldt, J., Freitas, B., Galeazzi, C.,
594 Huizinga, R., Lanniruberto, M., Ma, H.B., Nittrouer, J.A., Oberg, K., Orfeo, O., Parsons,
595 D., Szupiany, R., Wang, P., Zhang, Y.F., 2020. Dunes in the world's big rivers are
596 characterized by low-angle lee-side slopes and a complex shape. Nature geoscience 13,
597 156-162.

598 Coastal Protection and Restoration Authority., 2017. Louisiana's comprehensive master plan for
599 a sustainable coast, Rep. (pp. 188), Coastal Protection and Restoration Authority of
600 Louisiana, Baton Rouge, LA.
601 Couvillion, B.R., Barras, J.A., Steyer, G.D., Sleavin, W., Fischer, M., Beck, H., et al., 2011.
602 Land area change in coastal Louisiana from 1932 to 2010: U.S. Geological Survey
603 Scientific Investigations Map 3164, pamphlet Rep. (pp. 12).
604 Das, H.S., Imran, J., Pirmez, C., Mohrig, D., 2004. Numerical modeling of flow and bed
605 evolution in meandering submarine channels. Journal of Geophysical Research 109, 1-17.
606 Duan, J.G., Julien, P.Y., 2010. Numerical simulation of meandering evolution. Journal of
607 Hydrology 391, 34-46.
608 Gualtieri, C., Ianniruberto, M., Filizola, N., Santos, R., Endreny, T., 2017. Hydraulic complexity
609 at a large river confluence in the Amazon basin. Ecohydrology 10, e1863.
610 He, L., 2018. Distribution of primary and secondary currents in sine-generated bends. Water SA
611 44, 118-129.
612 Hsieh, T.Y., Yang, J.C., 2003. Investigation on the suitability of two-dimensional depth-
613 averaged models for bend-flow simulation. Journal of Hydraulic Engineering 129, 597-
614 612.
615 Hu, Y.Y., 2005. Quantifying bedform migration using multi-beam sonar. Geo-Mar Lett 25, 306-
616 314.
617 Johannesson, H., Parker, G., 1989. Velocity redistribution in meandering rivers. Journal of
618 Hydraulic Engineering 115, 1019-1039.

619 Joshi, S., Xu, Y.J., 2015. Assessment of Suspended Sand Availability under Different Flow
620 Conditions of the Lowermost Mississippi River at Tarbert Landing during 1973–2013.
621 Water 7, 7022-7044.
622 Joshi, S., Xu, Y.J., 2017. Bedload and suspended load transport in the 140 km reach downstream
623 of the Mississippi River avulsion to the Atchafalava River. Water 9 (9), 716.
624 Karim, F., 1995. Bed configuration and hydraulic resistance in alluvial-channel flows. Journal of
625 Hydraulic Engineering-ASCE, 121 (1), 15-25.
626 Karim, F., 1999. Bed-form geometry in san-bed flows. Journal of Hydraulic Engineering, ASCE
627 125, 1253-1261.
628 Knaapen, M.A.F., Hulscher, S.J.M.H., Vriend, H.J., Stolk, A., 2001. A new type of sea bed
629 waves. Geophysical Research Letters 28, 1323-1326.
630 Knaapen, M.A.F., 2005. Sandwave migration predictor based on shape information. Journal of
631 Geophysical Research, 110, 1-9.
632 Knox, R.L., Latrubesse, E.M., 2016. A geomorphic approach to the analysis of bedload and bed
633 morphology of the Lower Mississippi River near the Old River Control Structure.
634 Geomorphology 268, 35-47.
635 Kondolf, G.M., 2006. River restoration and meanders. Ecology and Society 11 (2): Article
636 Number: 42.
637 Konsoer, K.M., Rhoads, B.L., Best, J.L., Langendoen, E.J., Abad, J.D., Parsons, D.R., Garcia,
638 M.H., 2016. Three-dimensional flow structure and bed morphology in large elongate
639 meander loops with different outer bank roughness characteristics. Water Resour. Res 52,
640 9621-9641.

641 Kostaschuk, R.A., Villard, P.V., 1996. Flow and sediment transport over large subaqueous
642 dunes: Fraser River, Canada. Sedimentology 43, 849-863.
643 Kozarek, J., Hession, W., Dolloff, C., Diplas, P., 2010. Hydraulic complexity metrics for
644 evaluating in-stream brook trout habitat. J. Hydraul. Eng 136, 1067-1076.
645 Leopold, L.B., Wolman, M.G., 1960. River meanders. Bull. Geol. Soc. Am 71, 769-793.
646 Li, W.H., Cheng, H.Q., Li, J.F., Dong, P., 2008. Temporal and spatial changes of dunes in the
647 Changjiang (Yangtze) Estuary, China. Estuarine, Coastal and Shelf Science 77, 169-174.
648 Liu, X.X., Bai, Y.C., 2014. Turbulent structure and bursting process in multi-bend meander
649 channel. Journal of Hydrodynamics 26, 207-215.
650 Lorenz, A.W., Jaehnig, S.C., Hering, D., 2009. Re-Meandering German Lowland Streams:
651 Qualitative and Quantitative Effects of Restoration Measures on Hydromorphology and
652 Macroinvertebrates. Environmental Management 44 (4), 745-754.
653 Maddux, T.B., Nelson, J.M., McLean, S.R., 2003. Turbulent flow over three-dimensional dunes
654 1. Free surface and flow response, J. Geophys, Res, 108 (F1), 6009.
655 McCoy, E.D., Bell, S.S., Mushinsky, H.R., 1999. Habitat structure: Synthesis and perspectives.
656 In Habitat Structure; Springer: Berlin, Germany, pp. 427-430.
657 Meade, R.H., Moody, J.A., 2010. Causes for the decline of suspended-sediment discharge in the
658 Mississippi River system, 1940–2007. Hydrological Processes 24, 35-49.
659 Milliman, J.D., Farnsworth, K.L., 2011. River Discharge to the Coastal Ocean: A Global
660 Synthesis. Cambridge University Press, New York.
661 Mossa, J., 1996. Sediment dynamics in the lowermost Mississippi River. Eng. Geol. 45, 457-479.

662 Naqshband, S., Ribberink, J.S., Hulscher, S.J.M.H., 2014. Using both free surface effect and
663 sediment transport mode parameters in defining the morphology of river dunes and their
664 evolution to upper stage plane beds. Journal of Hydraulic Engineering 140 (6), 06014010.
665 Naqshband, S., Duin, O., Ribberink, J., Hulscher, S., 2016. Modeling river dune development
666 and dune transition to upper stage plane bed. Earth Surface Processes and Landforms 41,
667 323-335.
668 Nittrouer. J.A., Allison, M.A., Campanella, R., 2008. Bedform transport rates for the lowermost
669 Mississippi River. Journal of Geophysical Research 113, 1-16.
670 Nittrouer, J.A., Mohrig, D., Allison, M., 2011a. Punctuated sand transport in the lowermost
671 Mississippi River. Journal of Geophysical Research 116, 1-24.
672 Nittrouer, J.A., Mohrig, D., Allison, M.A., Peyret, A.B., 2011b. The lowermost Mississippi
673 River: A mixed bedrock-alluvial channel. Sedimentology 58, 1914-1934.
674 Nittrouer, J.A., Shaw, J., Lamb, M.P., Mohrig, D., 2012. Spatial and temporal trends for water-
675 flow velocity and bed-material sediment transport in the lower Mississippi River. GSA
676 Bulletin 124, 400-414.
677 Odgaard, A.J., Bergs, M.A., 1988. Flow processes in a curved alluvial channel. Water Resources
678 Research 24, 45-56.
679 Paarlberg, A.J., Dohmen-Janssen, C.M., Hulscher, S.J.M.H., Termes, P., Schielen, R., 2010.
680 Modelling the effect of time-dependent river dune evolution on bed roughness and stage.
681 Earth Surf. Processes Landforms 35, 1854-1866.
682 Palmer, M.A., Menninger, H.L., Bernhardt, E., 2010. River restoration, habitat heterogeneity and
683 biodiversity: a failure of theory or practice? Freshwater Biology 55, 205-222.

684 Parsons, D.R., Best, J.L., Orfeo, O., Hardy, R.J., Kostaschuk, R., Lane, S.N., 2005. Morphology
685 and flow fields of three-dimensional dunes, Rio Parana, Argentina: Results from
686 simultaneous multibeam echo sounding and acoustic Doppler current profiling. Journal of
687 Geophysical Research 110, F04S03.
688 Ramirez, M.T., Allison, M.A., 2013. Suspension of bed material over sand bars in the Lower
689 Mississippi River and its implications for Mississippi delta environmental restoration.
690 Journal of Geophysical Research: Earth Surface118, 1085-1104.
691 Rosen, T., Xu, Y.J., 2014. A hydrograph-based sediment availability assessment: Implications
692 for Mississippi River sediment diversion. Water 6, 564-583.
693 Smith, J.D., McLean, S.R., 1977. Spatially averaged flow over a wavy surface. Journal of
694 Geophysical Research 82, 1735-1746.
695 Smith, J.D., McLean, S.R., 1984. A model for flow in meandering streams. Water Resources
696 Research 20, 1301-1315.
697 Southard, J.B., Boguchwal, A.L., 1990. Bed configurations in steady unidirectional water flows.
698 Part 2. Synthesis of flume data. Journal of Sedimentary Research 60, 658-679.
699 Syvitski, J.P.M., Milliman, J.D., 2007. Geology, geography, and humans battle for dominance
700 over the delivery of fluvial sediment to the coastal ocean. Journal of Geology 115, 1-19.
701 Termini, D., Piraino, M., 2011. Experimental analysis of cross-sectional flow motion in a large
702 amplitude meandering bend. Earth Surface Processes and Landforms 36, 244-256.
703 Unsworth, C.A., Nicholas, A.P., Ashworth, P.J., Best, J.L., Lane, S.N., Parsons, D.R., Smith,
704 G.H.S., Simpson, C.J., Strick, R.J.P., 2020. Influence of Dunes on Channel-Scale Flow
705 and Sediment Transport in a Sand Bed Braided River. Journal of Geophysical Research:
706 Earth Surface,125, e2020JF005571. https://doi.org/10.1029/2020JF005571.

Van Rijn, L.C., 1984. Sediment transport, part III: Bed forms and alluvial roughness. Journal of Hydraulic Engineering 110, 1733-1754.

Vermeulen, B., Hoitink, A.J.F., Labeur, R.J., 2015. Flow structure caused by a local cross-sectional area increase and curvature in a sharp river bend. J. Geophys. Res. Earth Surf 120, 1771-1783, doi:10.1002/2014jf003334.

Vorosmarty, C.J., Meybeck, M., Fekete, B., Sharma, K., Green, P., Syvitski, J.P.M., 2003. Anthropogenic sediment retention: major global impact from registered river impoundments. Global and Planetary Change 39 (1-2), 169-190.

Walling, D.E., Fang, D., 2003. Recent trends in the suspended sediment loads of the world's rivers. Global and Planetary Change 39 (1-2), 111-126.

Walling, D.E., 2006. Human impact on land-ocean sediment transfer by the world's rivers. Geomorphology 79 (3-4), 192-216.

Wang, B., Xu, Y.J., 2015. Sediment Trapping by Emerged Channel Bars in the Lowermost Mississippi River during a Major Flood. Water 7, 6079-6096.

Wang, B., Xu, Y.J., 2016. Long-term geomorphic response to flow regulation in a 10-km reach downstream of the Mississippi - Atchafalaya River diversion. Journal of Hydrology: Regional Studies 8, 10-25.

Wang, B., Xu, Y.J., 2018. Decadal-Scale Riverbed Deformation and Sand Budget of the Last 500 km of the Mississippi River: Insights into natural and river engineering effects on a large alluvial river. Journal of Geophysical Research: Earth Surface 123, 1-17.

Wang, B., Xu, Y.J., 2020. Estimating bed material fluxes upstream and downstream of a controlled large bifurcation - the Mississippi-Atchafalaya River diversion. Hydrological Processes doi: 10.1002/hyp.13771.

730 Wilson, K.N., Baker, S.L., Kondolf, G.M., 2020. The ideal meander: Exploring freshwater
731 scientist drawings of river restoration. Freshwater Science 39 (2), 349-355.
732 Winkley, B.R., 1977. Man-made cuoffs on the lower Mississippi River, conception, construction,
733 and river response. Potamology Investigations Report 300-2, U.S. Army Corps of
734 Engineers, Vicksburg, Mississippi, pp 209.
735 Wohl, E., 2020. Rivers in the Landscape; JohnWiley & Sons: Hoboken, NJ, USA.
736 Wu, Z.Y., Jin, X.L., Li, J.B., 2005. Linear sand ridges on the outer shelf of the East China Sea.
737 China Sci. Bull 50, 2517-2528. (In Chinese)
738 Wu, J.X., Wang, Y.H., Cheng, H.Q., 2009. Bedforms and bed material transport pathways in the
739 Changjiang (Yangtze) Estuary. Geomorphology 104, 175-184.
740 Wu, Z.Y., Jin, X.L., Cao, Z Y., Li, J.B., Zheng, Y.L., Shang, J.H., 2010. Distribution, formation
741 and evolution of sand ridges on the East China Sea shelf. Science China Earth Sciences
742 53, 101-112.
743 Wu, S.H., Cheng, H.Q., Xu, Y.J., Li, J.F., Zheng, S.W., Xu, W., 2016. Riverbed
744 Micromorphology of the Yangtze River Estuary, China. Water 8, 190.
745 Wu, C.L., Nittrouer, J.A., Swanson, T., Ma, H.B., Barefoot, E., Best, J., Allison, M., 2020.
746 Dune-scale cross-strata across the fluvial-deltaic backwater regime: Preservation
747 potential of an autogenic stratigraphic signature. Geology 48, 1-5.
748 Zheng, S.W., Cheng, H.Q., Wu, S.H., Shi, S.Y., Xu, W., Zhou, Q.P., Jiang, Y.H., 2017.
749 Morphology and mechanism of the very large dunes in the tidal reach of the Yangtze
750 River, China. Continental Shelf Research 139, 54-61.
751 Zhou, T., Endreny, T., 2020. The Straightening of a River Meander Leads to Extensive Losses in
752 Flow Complexity and Ecosystem Services. Water, doi:10.3390/w12061680.

753

754

755

756

757

758

759

760

761

762

763

764

765

766

767

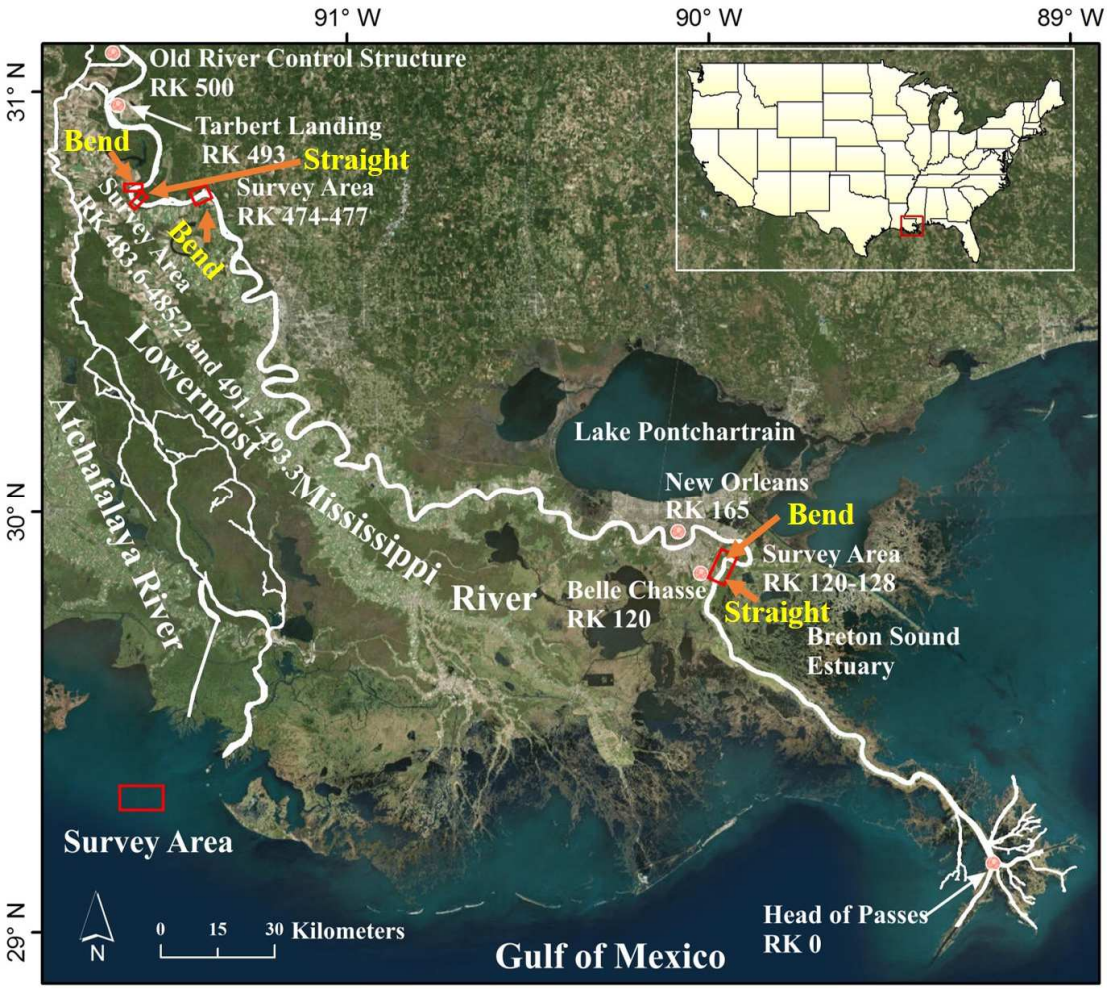
91° W
90° W
89° W
31° N
30° N
29° N
Old River Control Structure
RK 500
Tarbert Landing
RK 493
Bend
Straight
Survey Area
RK 474-477
Bend
Survey Area
RK 483.6-485.2 and 491.7-493.3
Lowermost Mississippi River
Atchafalaya River
Lake Pontchartrain
New Orleans
RK 165
Bend
Survey Area
RK 120-128
Belle Chasse
RK 120
Straight
Breton Sound
Estuary
Survey Area
N
0 15 30 Kilometers
Gulf of Mexico
Head of Passes
RK 0

Figure 1

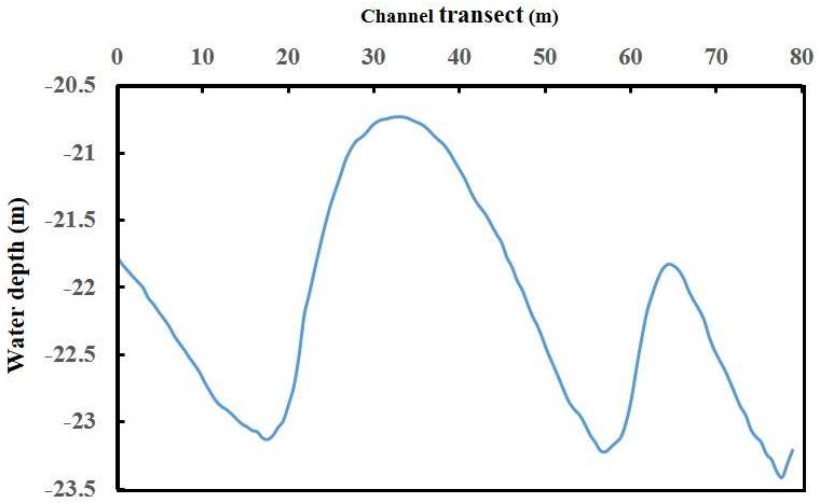
Channel transect (m)
0
10
20
30
40
50
60
70
80
Water depth (m)
-20.5
-21
-21.5
-22
-22.5
-23
-23.5

Figure 2

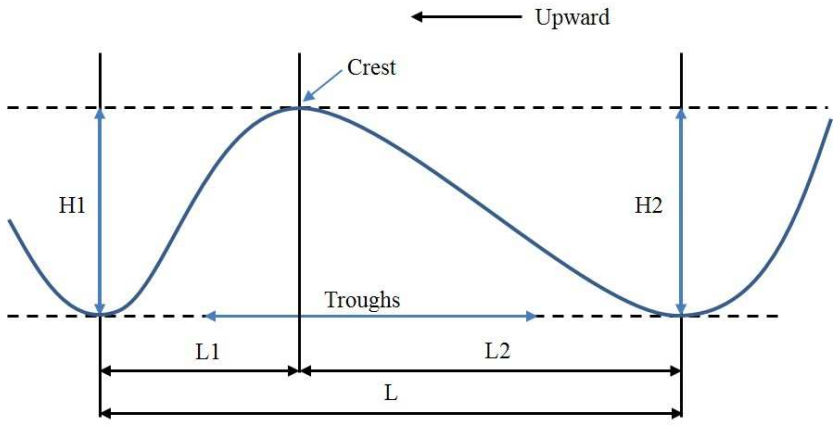

Figure 3

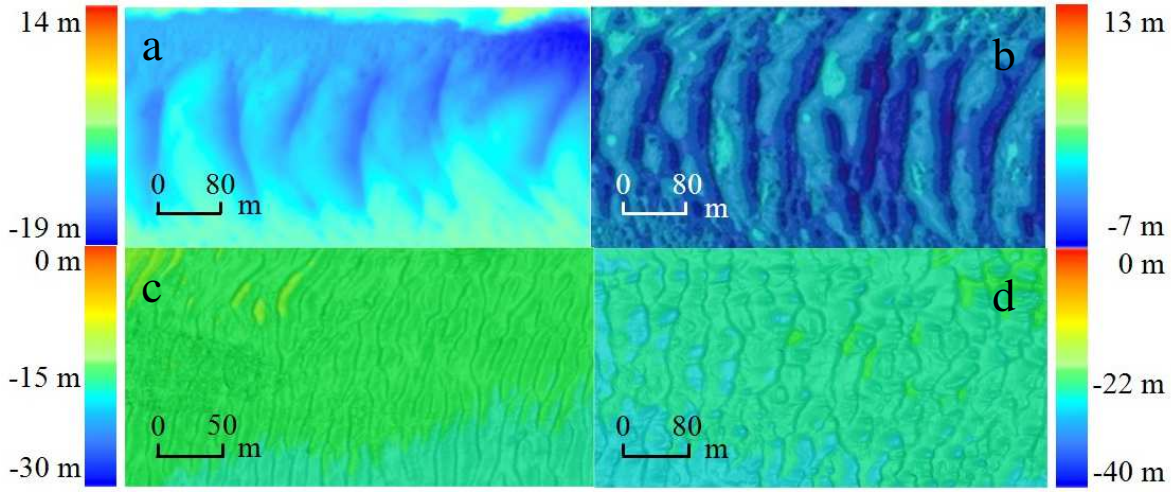

Figure 4

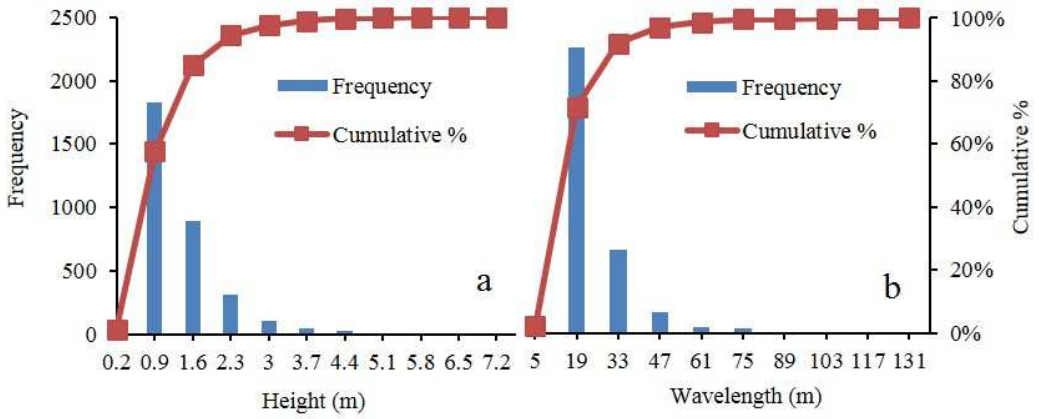
2500
2000
1500
1000
500
0
Frequency
Frequency
Cumulative %
a
0.2 0.9 1.6 2.3 3 3.7 4.4 5.1 5.8 6.5 7.2
Height (m)
100%
80%
60%
40%
20%
0%
Cumulative %
Frequency
Cumulative %
b
5 19 33 47 61 75 89 103 117 131
Wavelength (m)

Figure 5

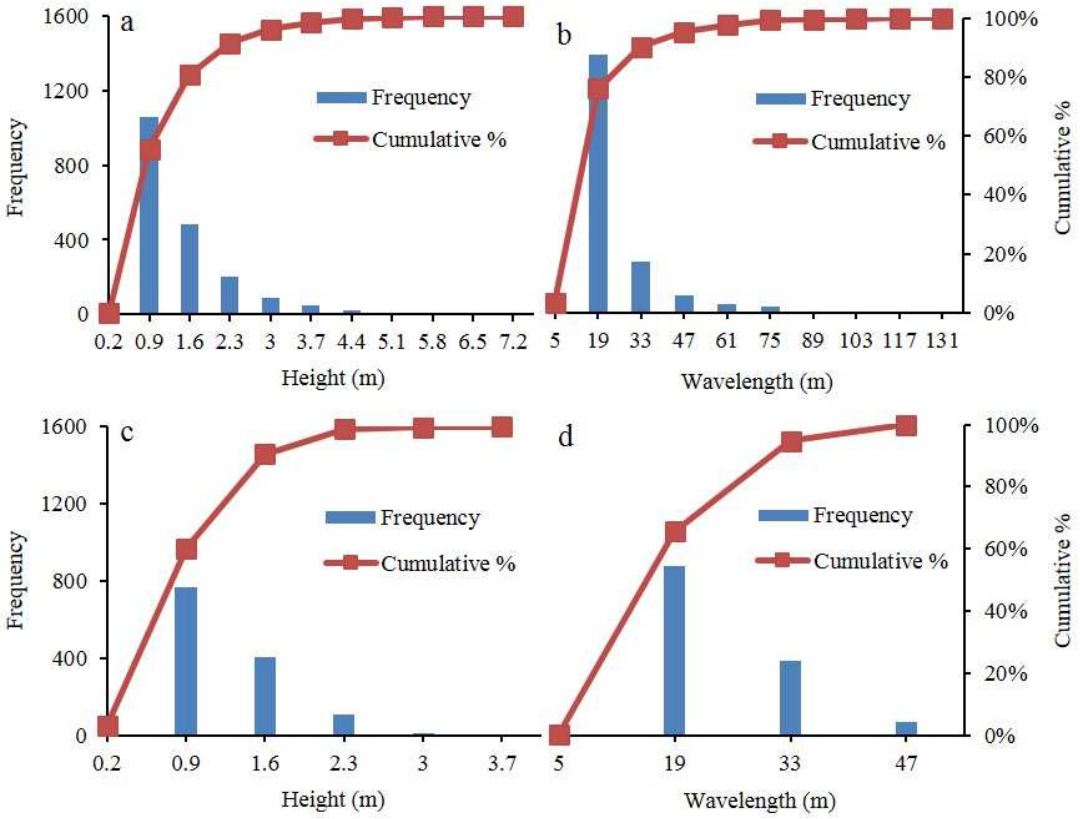
a
b
c
d
Frequency
Cumulative %
Height (m)
Wavelength (m)
Cumulative %
1600
1200
800
400
0
100%
80%
60%
40%
20%
0%
0.2 0.9 1.6 2.3 3 3.7 4.4 5.1 5.8 6.5 7.2
5 19 33 47 61 75 89 103 117 131

Figure 6

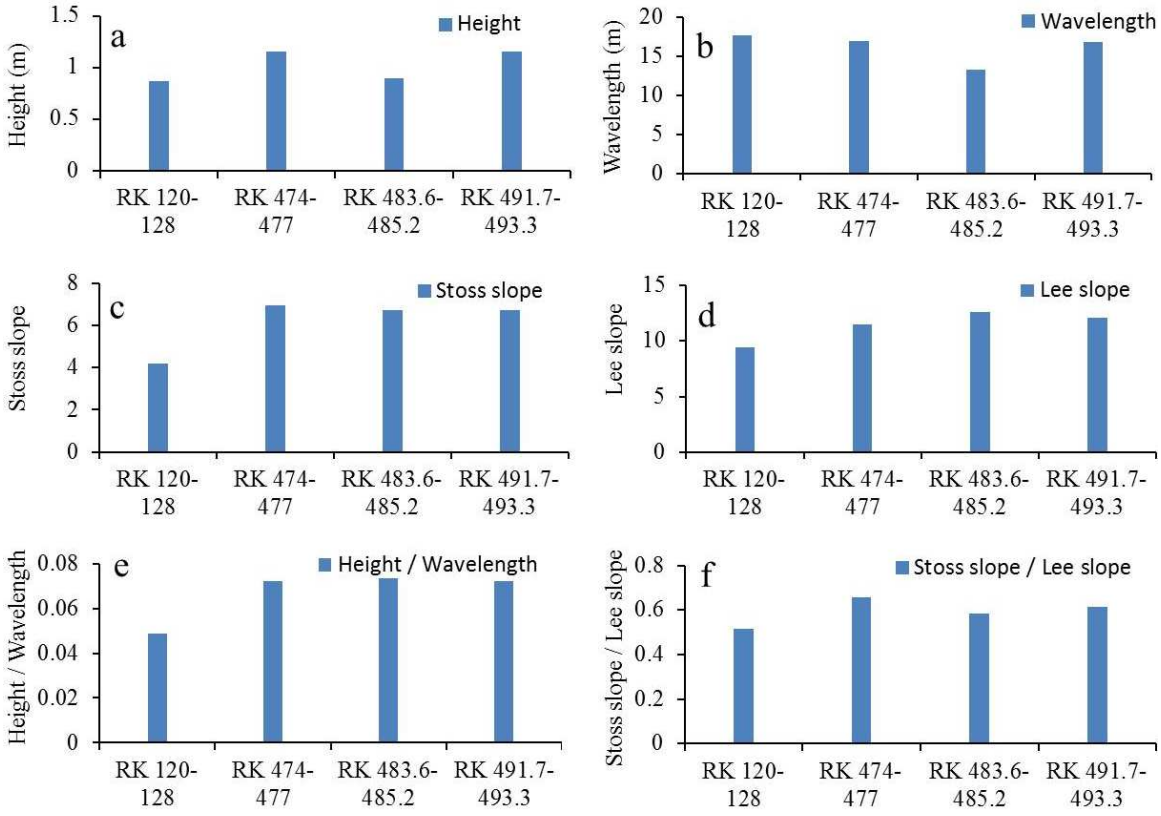
a
Height
Height (m)
1.5
1
0.5
0
RK 120-128
RK 474-477
RK 483.6-485.2
RK 491.7-493.3
b
Wavelength
Wavelength (m)
20
15
10
5
0
c
Stoss slope
8
6
4
2
d
Lee slope
e
Height / Wavelength
0.08
0.06
0.04
0.02
f
Stoss slope / Lee slope
0.8
0.6
0.4
0.2

Figure 7

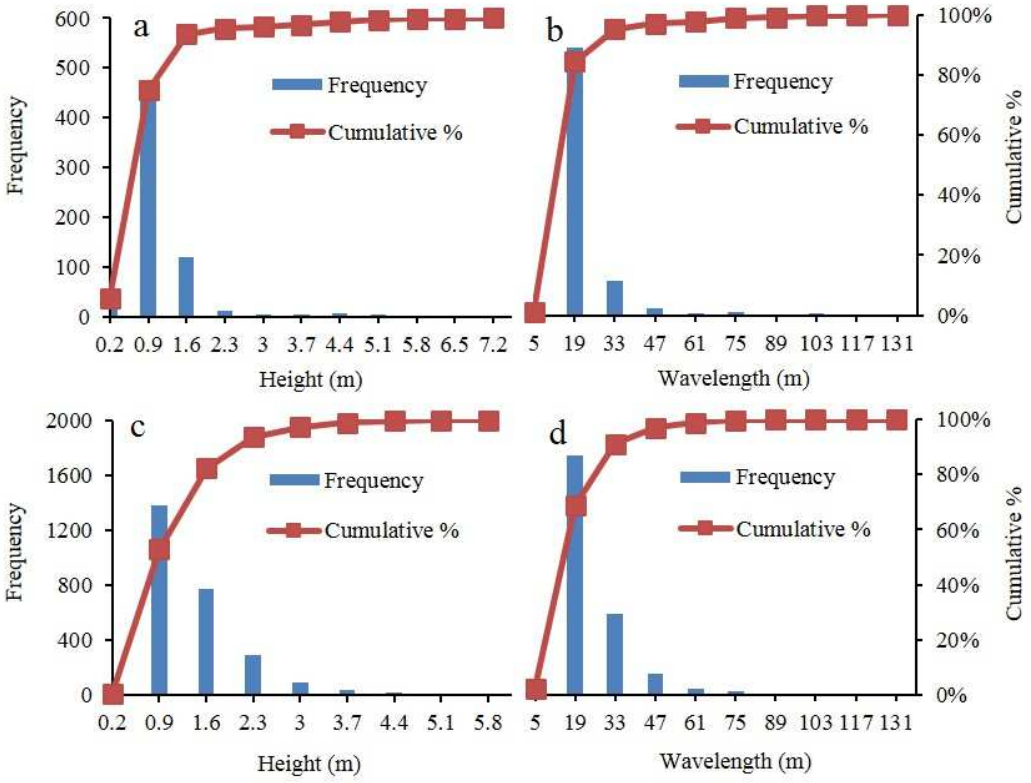
a
b
c
d
Frequency
Cumulative %
Cumulative %
Height (m)
Wavelength (m)
0.2 0.9 1.6 2.3 3 3.7 4.4 5.1 5.8 6.5 7.2
5 19 33 47 61 75 89 103 117 131
0.2 0.9 1.6 2.3 3 3.7 4.4 5.1 5.8
0 100 200 300 400 500 600
0 400 800 1200 1600 2000
0% 20% 40% 60% 80% 100%

Figure 8

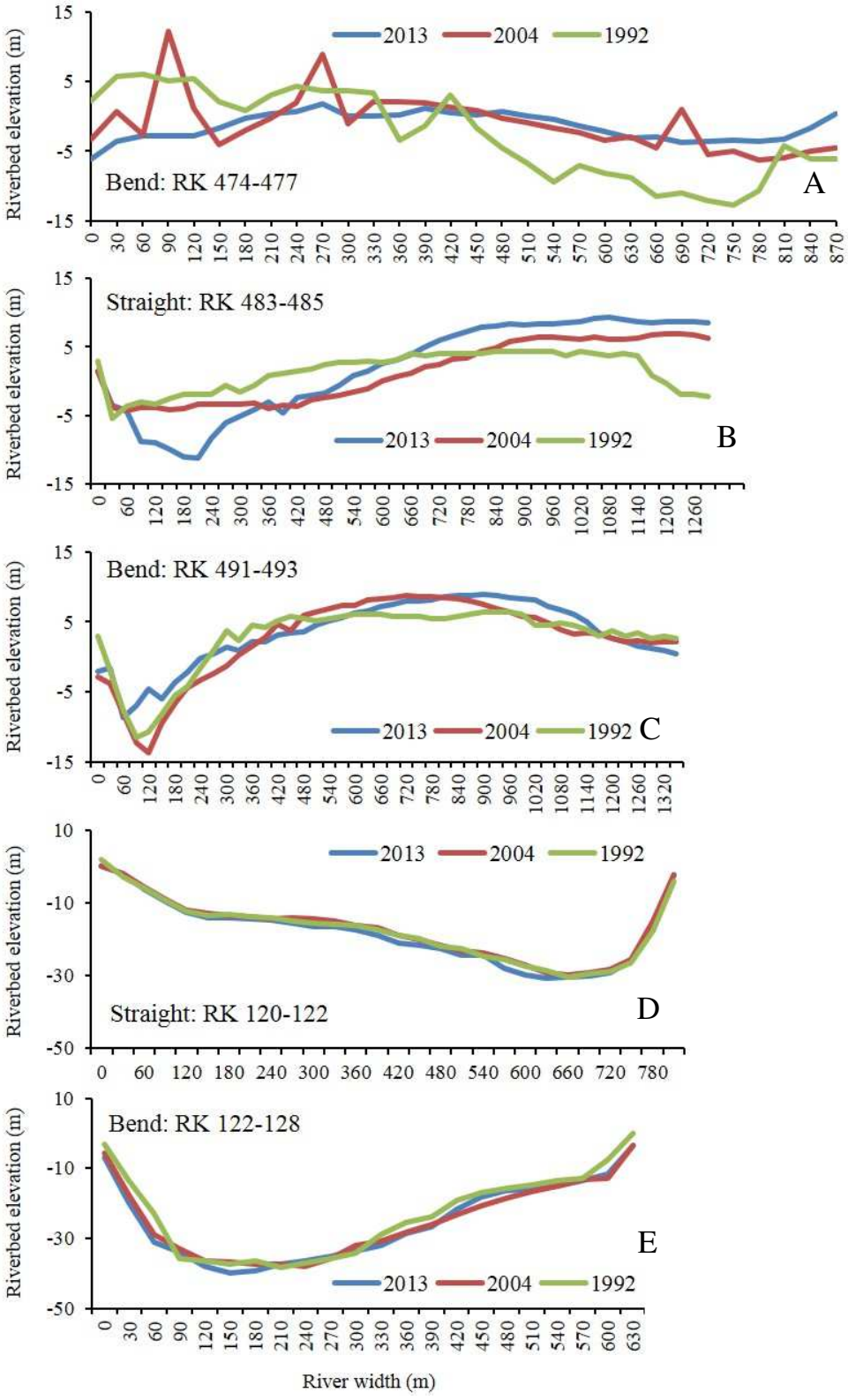
Riverbed elevation (m)
2013
2004
1992
Bend: RK 474-477
A
Straight: RK 483-485
B
Bend: RK 491-493
C
Straight: RK 120-122
D
Bend: RK 122-128
E
River width (m)

Figure 9

888 **Table 1**. Characteristics of five study river reaches of the Lowermost Mississippi River. The channel
889 width was calculated using multi-beam sonar survey data that covered the entire river channel.

	RK 120-122	RK 122-128	RK 474-477	RK 483.6-485.2	RK 491.7-493.3
Length (m)	2000	6000	3000	1600	1600
Width (m)	815	635	875	1300	1370
Depth (m)	0.5--33	0.35--46	14--11	14--19	14--7.5
Sinuosity	1.01	1.14	1.16	1.01	1.14
Shape	Straight reach	Bend	Bend	Straight reach	Bend

890
891
892
893
894
895
896
897
898
899
900
901
902
903
904
905

Table 2. Mean/median grain size of bed sediment in the Lowermost Mississippi River (unit: μm).

	2012[a]	2003-2004[b]	2003-2004[b]	2010[c]	2008[d]	2003-2004[b]
Reach	RK 396-511	RK 162-167	RK 132-140	RK 75-100	RK 35-50	RK 7-12
Mean grain size		275	260	225		175
Median grain size	181-483			150-350	166-266	

Note: the original data of *[a] from Knox and Latrubesse, 2016; [b] from Nittrouer et al., 2008; [c] from Ramirez and Allison, 2013; [d] from Nittrouer et al., 2011a.*

925 **Table 3**. Characteristic difference in dunes in different river reaches of the Lowermost Mississippi
926 River.

Region (number of dunes)	**Height (m)**		**Length (m)**		**Stoss side angle** (°)		**Lee side angle** (°)		**Roughness**
	Max.	Mean	Max.	Mean	Max.	Mean	Max.	Mean	Mean
Straight reach (642)	6.69	0.81	129.54	14.27	17.75	5.48	42.23	10.28	0.68
Bend (2616)	5.17	1.06	117.65	17.40	31.64	5.83	47.11	10.93	0.91
Upper reach (1928)	6.69	1.11	129.54	16.21	17.51	6.89	47.11	11.79	1
Lower reach (1330)	3.16	0.87	46.02	17.62	31.64	4.21	44.44	9.36	0.68
Study reach (3258)	6.69	1.01	129.54	16.79	31.64	5.76	47.11	10.8	

927
928
929
930
931
932
933
934
935
936
937
938
939
940

941

942 **Table 4.** Comparison of dune size in the upper/lower reaches of the Lowermost Mississippi River.

Variables	Groups	Mean	Standard deviation	N	p-value
Height	Upper reach	1.11	0.68	1330	<0.0001*
	Lower reach	0.87	0.23		
Wavelength	Upper reach	16.21	209.64	1330	0.0007*
	Lower reach	17.62	62.31		
Height/Wavelength	Upper reach	0.073	0.0004	1330	<0.0001*
	Lower reach	0.049	0.0003		
Stoss side slope	Upper reach	6.92	4.78	1330	<0.0001*
	Lower reach	4.21	3.23		
Leeside slope	Upper reach	11.77	27.26	1330	<0.0001*
	Lower reach	9.40	21.12		
Stoss slope/Lee slope	Upper reach	0.64	0.05	1330	<0.0001*
	Lower reach	0.52	0.07		

943 *Statistically significant.

944

945

946

947

948

949

950

951

952

953 **Table 5.** Comparison of dune size in the straight reaches/bends of the Lowermost Mississippi River.

Variables	Groups	Mean	Standard deviation	N	p-value
Height	Straight reach	0.81	0.56	642	<0.0001*
	Bend	1.06	0.26		
Wavelength	Straight reach	14.27	171.05	642	<0.0001*
	Bend	17.40	71.52		
Height/wavelength	Straight reach	0.060	0.0006	642	<0.0001*
	Bend	0.052	0.0004		
Stoss side slope	Straight reach	5.48	5.85	642	<0.0001*
	Bend	4.41	4.36		
Leeside slope	Straight reach	10.45	34.18	642	0.54
	Bend	10.27	22.87		
Stoss slope/Lee slope	Straight reach	0.61	0.098	642	<0.0001*
	Bend	0.48	0.039		

954 *Statistically significant.

955

956

957

958

959

960

961

962

963 **Table 6**. Characteristics of dunes in straight reaches and meandering bends of the upper and lower

964 Lowermost Mississippi River for different water depths (note: water depths are negative).

Region	**Water depth**	**Height (m)**		**Length (m)**		**Stoss side angle (°)**		**Lee side angle (°)**		**Roughness**
		Max.	Mean	Max.	Mean	Max.	Mean	Max.	Mean	Mean
Straight reach (RK 121-122)	18.5-25.5	1.14	0.53	21.03	11.58	6.24	3.84	22.01	8.54	0.40
	26-30	2.4	1.02	39.01	19.74	17.75	4.84	39.33	10.01	0.81
Meander bend (RK 126.6-127.6)	17-19	2.22	1.29	42.98	29.33	6.65	4.05	12.46	7.23	0.95
	19-22	2.05	1.26	38.40	25.09	11.12	4.37	23.80	9.68	0.90
	23-25	1.85	1.05	36.27	20.16	8.24	4.31	24.60	10.83	0.84
	25-27	1.94	0.64	27.74	13.7	6.77	3.89	19.96	8.64	0.49

965